



City Research Online

City, University of London Institutional Repository

Citation: Favier, J., Revell, A. & Pinelli, A. (2016). Fluid Structure Interaction of Multiple Flapping Filaments Using Lattice Boltzmann and Immersed Boundary Methods. *Advances in fluid structure interaction*, 133, pp. 167-178. doi: 10.1007/978-3-319-27386-0_10

This is the accepted version of the paper.

This version of the publication may differ from the final published version.

Permanent repository link: <https://openaccess.city.ac.uk/id/eprint/17708/>

Link to published version: https://doi.org/10.1007/978-3-319-27386-0_10

Copyright: City Research Online aims to make research outputs of City, University of London available to a wider audience. Copyright and Moral Rights remain with the author(s) and/or copyright holders. URLs from City Research Online may be freely distributed and linked to.

Reuse: Copies of full items can be used for personal research or study, educational, or not-for-profit purposes without prior permission or charge. Provided that the authors, title and full bibliographic details are credited, a hyperlink and/or URL is given for the original metadata page and the content is not changed in any way.

City Research Online:

<http://openaccess.city.ac.uk/>

publications@city.ac.uk

Metadata of the chapter that will be visualized in SpringerLink

Book Title	Advances in Fluid-Structure Interaction	
Series Title		
Chapter Title	Fluid Structure Interaction of Multiple Flapping Filaments Using Lattice Boltzmann and Immersed Boundary Methods	
Copyright Year	2016	
Copyright HolderName	Springer International Publishing Switzerland	
Corresponding Author	Family Name	Favier
	Particle	
	Given Name	Julien
	Prefix	
	Suffix	
	Division	
	Organization	Laboratoire de Mécanique, Modélisation et Procédés Propres (M2P2) Aix Marseille Université, CNRS UMR 7340
	Address	Centrale Marseille, France
	Email	Julien.Favier@univ-amu.fr
Author	Family Name	Revell
	Particle	
	Given Name	Alistair
	Prefix	
	Suffix	
	Division	
	Organization	School of Mechanical, Aerospace and Civil Engineering (MACE) University of Manchester
	Address	Manchester, UK
	Email	
Author	Family Name	Pinelli
	Particle	
	Given Name	Alfredo
	Prefix	
	Suffix	
	Division	School of Engineering and Mathematical Sciences
	Organization	City University
	Address	London, UK
	Email	

Abstract The problem of flapping filaments in an uniform incoming flow is tackled using a Lattice Boltzmann—Immersed Boundary method. The fluid momentum equations are solved on a Cartesian uniform lattice while the beating filaments are tracked through a series of markers, whose dynamics are functions of the forces exerted by the fluid, the filament flexural rigidity and the tension. The instantaneous wall conditions on the filament are imposed via a system of singular body forces, consistently discretised on the lattice of the Boltzmann equation. We first consider the case of a single beating filament, and then the case of

multiple beating filaments in a side-by-side configuration, focussing on the modal behaviour of the whole dynamical systems.

Keywords (separated by '-') Beating filaments - Immersed boundary - Lattice Boltzma - Flapping modes

Fluid Structure Interaction of Multiple Flapping Filaments Using Lattice Boltzmann and Immersed Boundary Methods

Julien Favier, Alistair Revell and Alfredo Pinelli

Abstract The problem of flapping filaments in an uniform incoming flow is tackled using a Lattice Boltzmann—Immersed Boundary method. The fluid momentum equations are solved on a Cartesian uniform lattice while the beating filaments are tracked through a series of markers, whose dynamics are functions of the forces exerted by the fluid, the filament flexural rigidity and the tension. The instantaneous wall conditions on the filament are imposed via a system of singular body forces, consistently discretised on the lattice of the Boltzmann equation. We first consider the case of a single beating filament, and then the case of multiple beating filaments in a side-by-side configuration, focussing on the modal behaviour of the whole dynamical systems.

Keywords Beating filaments · Immersed boundary · Lattice Boltzma · Flapping modes

1 Introduction

The dynamics of flapping filaments in a streaming ambient fluid covers a broadband range of applications (aeronautics, civil engineering, biological flows, etc.) and constitutes a challenging problem, from the theoretical and numerical point of view [1, 2]. In particular, the experiments in soap films performed by [3, 4] are very interesting in this context, as they can be considered as a reasonable approximation of

J. Favier (✉)

Laboratoire de Mécanique, Modélisation et Procédés Propres (M2P2)
Aix Marseille Université, CNRS UMR 7340, Centrale Marseille, France
e-mail: Julien.Favier@univ-amu.fr

A. Revell

School of Mechanical, Aerospace and Civil Engineering (MACE)
University of Manchester, Manchester, UK

A. Pinelli

School of Engineering and Mathematical Sciences, City University, London, UK

© Springer International Publishing Switzerland 2016

M. Braza et al. (eds.), *Advances in Fluid-Structure Interaction*,
Notes on Numerical Fluid Mechanics and Multidisciplinary Design 133,
DOI 10.1007/978-3-319-27386-0_10

1

19 2D fluid structure interaction scenarios, thus suitable for the validation of the results
20 obtained with our numerical approach. In our simulations, we consider a 2D incom-
21 ing incompressible flow modeled through a Lattice Boltzmann method, coupled to
22 a model of infinitely thin and inextensible filaments experiencing tension, gravity,
23 fluid forces and flexural rigidity (i.e. a bending term in the form of a 4th derivative
24 with respect to the curvilinear coordinate describing the filament). Also, at all time
25 instants tension forces are determined to maintain the inextensibility of the structure.
26 In this simple model the energy balance of the system is driven by the bending forces
27 and fluid forces, as the structure is controlled by an inextensibility constraint which
28 prohibits stretching or elongation motions that would dissipate energy. This system
29 encompasses all the essential ingredients of a complex fluid-structure interaction
30 problem: large deformations, slender flexible body, competition between bending
31 versus fluid forces, inextensibility and effect of the filament tips on the surrounding
32 flow as vorticity generators.

33 To enforce the presence of the solid on the fluid lattice, we use a variant of the
34 immersed boundary method previously developed by the authors [5]. This approach is
35 efficient, accurate, computationally cheap and directly provides for the forces exerted
36 on the fluid by the filaments without the introduction of any empirical parameter.
37 Using the Lattice Boltzmann method in conjunction with an Immersed Boundary
38 technique to solve the motion of an incompressible fluid also allows for a clean
39 imposition of the boundary conditions on the solid since it does not suffer from
40 errors originating from the projection step associated with unsteady incompressible
41 Navier Stokes solvers [6].

42 Making use of the outlined Lattice Boltzmann—Immersed Boundary approach,
43 we consider the coupled dynamics of systems made of flapping filaments placed
44 side-by-side in an uniform incoming flow. No artificial contact force is introduced
45 between the filaments to keep a purely hydrodynamical interaction between fila-
46 ments. The ultimate aim of the simulations concerns the dynamical characterisation
47 of the collective behavior of a set of filaments and their potential use as a deforming
48 actuator for the control of fluid flows. In particular, the modal behavior of the system,
49 that mainly depends on the filament spacings [7, 8], could be envisaged either as an
50 *unsteady* generator of vortical structures, able to energize locally boundary layers
51 on the verge of separation (thus delaying their detachment), or to control the wake
52 behind bluff bodies [9].

53 2 Coupled Lattice Boltzmann—Immersed Boundary 54 Method

55 The fluid-structure problem involving the mutual interaction between moving flexible
56 objects and a surrounding fluid flow is tackled using an Immersed Boundary method
57 coupled with a Lattice Boltzmann solver. In the following we will just present brief
58 highlights on the numerical techniques entering in the whole numerical formulation.
59 More details about the numerical methodology can be found in [10].

60 The fluid flow is modeled by advancing in time the Lattice Boltzmann equation
 61 which governs the transport of particles density distribution f (probability of finding
 62 a particle in a certain location with a certain velocity). It is often classified as a
 63 mesoscopic method, where the macroscopic variables, namely mass and momentum,
 64 are derived from the distribution functions f . An excellent review of the method can
 65 be found in [11].

66 Using the classical BGK approach [12], the Boltzmann transport equation for the
 67 distribution function $f = f(\mathbf{x}, \mathbf{e}, t)$ at a node \mathbf{x} and at time t with particle velocity
 68 vector \mathbf{e} is given as follows:

$$69 \quad f_i(\mathbf{x} + \mathbf{e}_i \Delta t, t + \Delta t) - f_i(\mathbf{x}, t) = -\frac{\Delta t}{\tau} (f(\mathbf{x}, t) - f^{(eq)}(\mathbf{x}, t)) + \Delta t F_i \quad (1)$$

70 In this formulation, \mathbf{x} are the space coordinates, \mathbf{e}_i is the particle velocity in the
 71 i th direction of the lattice and F_i accounts for the body force applied to the fluid,
 72 which conveys the information between the fluid and the flexible structure. The local
 73 particles distributions relax to an equilibrium state $f^{(eq)}$ in a single time τ . Equation 1
 74 governs the collision of particles relaxing toward equilibrium (first term of the r.h.s.)
 75 together with their streaming which drives the data shifting between lattice cells (l.h.s.
 76 of the equation). The rate of approach to equilibrium is controlled by the relaxation
 77 time τ , which is related to the kinematic viscosity of the fluid by $\nu = (\tau - 1/2)/3$.
 78 This equation is solved on a cartesian uniform lattice. To each particle of each cell of
 79 the lattice a finite number of discrete velocity vectors are assigned. In particular, we
 80 use the D2Q9 model, which refers to two-dimensional and nine discrete velocities
 81 per lattice node (which corresponds to the directions east, west, north, south, center,
 82 and the 4 diagonal directions). In Eq. 1 the subscript i refers to these discrete particle
 83 directions. As it is usually done, a convenient normalization is used so that the
 84 spatial and temporal discretization in the lattice are set to unity, and thus the discrete
 85 velocities are defined as follows:

$$86 \quad \mathbf{e}_i = c \begin{pmatrix} 0 & 1 & -1 & 0 & 0 & 1 & -1 & 1 & -1 & 0 \\ 0 & 0 & 0 & 1 & -1 & 1 & -1 & -1 & 1 & 0 \end{pmatrix} \quad (i = 0, 1, \dots, 8) \quad (2)$$

87 where c is the lattice speed which defined by $c = \Delta x / \Delta t = 1$ with the current
 88 normalization. The equilibrium function $f^{(eq)}(\mathbf{x}, t)$ can be obtained by Taylor series
 89 expansion of the Maxwell-Boltzmann equilibrium distribution [13]:

$$90 \quad f_i^{(eq)} = \rho \omega_i \left[1 + \frac{\mathbf{e}_i \cdot \mathbf{u}}{c_s^2} + \frac{(\mathbf{e}_i \cdot \mathbf{u})^2}{2c_s^4} - \frac{\mathbf{u}^2}{2c_s^2} \right] \quad (3)$$

91 In Eq. 3, c_s is the speed of sound $c_s = 1/\sqrt{3}$ and the weight coefficient ω_i are $\omega_0 =$
 92 $4/9$, $\omega_i = 1/9$, $i = 1, \dots, 4$ and $\omega_5 = 1/36$, $i = 5, \dots, 8$ according to the current
 93 normalization. The macroscopic velocity \mathbf{u} in Eq. 3 must satisfy the requirement for
 94 low Mach number, M , i.e. that $|\mathbf{u}|/c_s \approx M \ll 1$. This stands as the equivalent
 95 of the CFL number for classical Navier Stokes solvers. The force F_i in Eq. 1 is

96 computed using a power series in the particle velocity with coefficients that depend
 97 on the actual volume force \mathbf{f}_{ib} applied on the fluid. The latter is determined using
 98 the Immersed Boundary method, following the formulation described in [10]. In this
 99 approach, the flexible filaments are discretised by a set of markers \mathbf{X}_k , that in general
 100 do not correspond with the lattice nodes $\mathbf{x}_{i,j}$. The role of \mathbf{f}_{ib} is to restore the desired
 101 velocity boundary values on the immersed surfaces at each time step.

102 The global algorithm is decomposed as follows. The Lattice-Boltzmann equations
 103 for the fluid are first advanced to the next time step without immersed object ($F_i = 0$),
 104 which provides the distribution functions f_i needed to build a predictive velocity \mathbf{u}^{P}
 105 by $\rho\mathbf{u}^{\text{P}} = \sum_i \mathbf{e}_i f_i$ and $\rho = \sum_i f_i$. The predictive velocity is then interpolated on the
 106 structure markers, which allows to derive the forcing required to impose the desired
 107 boundary condition at each marker using:

$$108 \quad \mathbf{F}_{\text{ib}}(\mathbf{X}_k) = \frac{\mathbf{U}^{\text{d}^{n+1}}(\mathbf{X}_k) - \mathcal{I}[\mathbf{u}^{\text{P}}](\mathbf{X}_k)}{\Delta t} \quad (4)$$

109 In Eq. 4, the term $\mathbf{U}^{\text{d}^{n+1}}(\mathbf{X}_k)$ denotes the velocity value at the location \mathbf{X}_k we wish
 110 to obtain at time step completion. It is determined by the motion equation of the
 111 filaments given by:

$$112 \quad \frac{d\mathbf{U}^{\text{d}^{n+1}}}{dt} = \frac{\partial}{\partial s} \left(T \frac{\partial \mathbf{X}_k}{\partial s} \right) - K_B \frac{\partial^4 \mathbf{X}_k}{\partial s^4} + Ri \frac{\mathbf{g}}{g} - \mathbf{F}_{\text{ib}} \quad (5)$$

113 Here, Ri is the Richardson number $Ri = gL/U_\infty^2$, T is the tension of the filament
 114 and K_B is the flexural rigidity. The closure of Eq. 5 is provided by the inextensibility
 115 condition that reads:

$$116 \quad \frac{\partial \mathbf{X}_k}{\partial s} \cdot \frac{\partial \mathbf{X}_k}{\partial s} = 1 \quad (6)$$

117 This condition basically ensures that the filament does not stretch, and thus its length
 118 remains constant. The boundary conditions are $\mathbf{X} = \mathbf{X}_0$, $\frac{\partial^2 \mathbf{X}_k}{\partial s^2} = 0$ for the fixed end
 119 and $T = 0$, $\frac{\partial^2 \mathbf{X}_k}{\partial s^2} = 0$ for the free end.

120 Coming back to Eq. 4, the term $\mathcal{I}[\mathbf{u}^{\text{P}}](\mathbf{X}_k)$ refers to the value of the predictive
 121 velocity field interpolated at \mathbf{X}_k . This basically provides the kinematic compatibility
 122 between solid and fluid motion, i.e. zero relative velocity on the solid boundary.
 123 At this stage, the required forcing is known at each marker by Eq. 4, and needs to
 124 be spread onto the lattice neighbours by: $\mathbf{f}_{\text{ib}}(\mathbf{x}) = \mathcal{S}(\mathbf{F}_{\text{ib}}(\mathbf{X}_k))$. More details on the
 125 interpolation operator \mathcal{I} , spreading operator \mathcal{S} and the filaments equations of motion
 126 can be found in [10]. The forcing \mathbf{f}_{ib} is finally discretised on the lattice directions
 127 using the series expansion suggested in [14]:

$$F_i = \left(1 - \frac{1}{2\tau}\right) \omega_i \left[\frac{\mathbf{e}_i - \mathbf{u}}{c_s^2} + \frac{\mathbf{e}_i \cdot \mathbf{u}}{c_s^4} \mathbf{e}_i \right] \cdot \mathbf{f}_{ib} \quad (7)$$

Equation 1 is then solved once again with the forcing F_i which impose the correct boundary condition at each marker \mathbf{X}_k . The macroscopic quantities are then derived from the obtained distribution functions f by $\rho \mathbf{u} = \sum_i \mathbf{e}_i f_i + \frac{\Delta t}{2} \mathbf{F}$ and $\rho = \sum_i f_i$, which closes one time step of the solver.

3 One Single Flapping Filament in an Incoming Fluid Flow

Following the experiments of [15], and the numerical study of [16], we start by considering the beating of a single filament fixed at one end, and subject to gravity and hydrodynamics forces. We fix the density difference between solid and fluid to $\Delta\rho = 1.5$, the non-dimensional bending rigidity to $K_B = 0.001$, and the value of the Richardson number to $Ri = 0.5$. The inlet velocity imposed in the Lattice-Boltzmann normalization is set to $U_\infty = 0.04$ (aligned with gravity direction), with a relaxation time of $\tau = 0.524$ and a filament length of $L = 40$. With these values, the simulation is run at a Reynolds number $Re = U_\infty L / \nu$ equal to 200. The size of the computational domain is set to $10L \times 15L$, in the transverse and streamwise direction respectively. The lattice discretization (600×400 nodes) has been determined as the result of a preliminary grid convergence study. The initial angle of the filament is set to $\theta = 18^\circ$ with respect to the gravity direction, and its fixed end is placed at the centerline of the domain, at a distance of $4L$ from the inlet. The L2 norm of the inextensibility error is kept below 10^{-12} systematically at all times.

Figure 1a shows the periodic pattern of the beating in the established regime, characterised by sinuous traveling waves moving and amplifying downstream from the fixed end. The same behavior has been observed both in the simulations of [17] and in the experiments of [2]. Figure 1b shows the time evolution of the y-coordinate (transverse direction) of the free end of the filament. After six beating cycles, a periodic orbit is established, with a period of 3 time units (the same value as the one

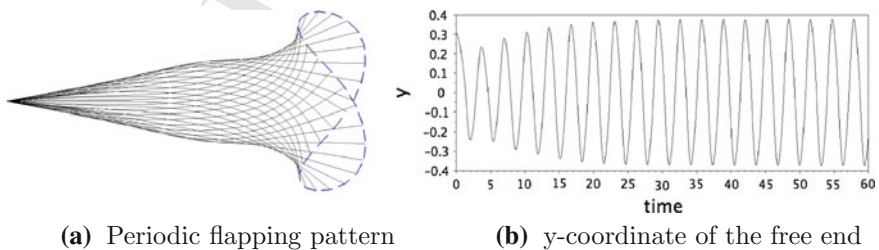


Fig. 1 Flapping motion of a single filament immersed in fluid at $Re = 200$, $Ri = 0.5$, $\Delta\rho = 1.5$. Fluid flows from left to right. **a** Beating pattern visualised by superimposed positions of the filament over one beating cycle. **b** Periodic time evolution of the y-coordinate of the free end

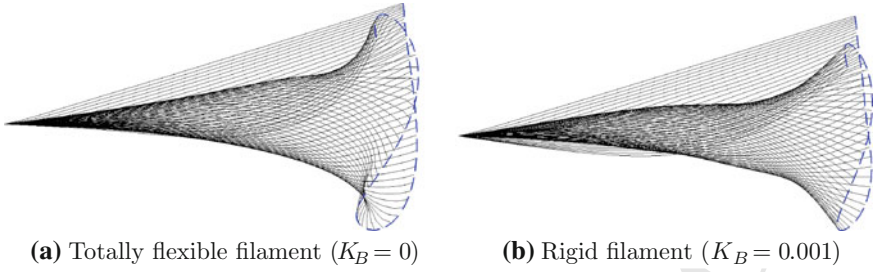


Fig. 2 Comparison between instantaneous snapshots of the flapping filament without bending (a) and with bending (b) starting from a straight initial configuration at an angle of $\theta_0 = 18^\circ$. The trajectory of the free end is shown in dashed line

154 found by [16]). The predicted amplitude of the beating compares well: the difference
 155 with reference data on the maximal excursion of the free end is less than 5%. Also,
 156 the peculiar trajectory of the free end exhibiting a characteristic *figure-eight* orbit
 157 (dashed line in Fig. 1a) is recovered, in agreement with the findings of the soap film
 158 experiments carried out by Zhang et al. [3].

159 Figure 2a, b show the effect of the bending rigidity coefficient on the beating
 160 pattern. Without bending rigidity (Fig. 2a), the filament is totally flexible and a rolling
 161 up of the free extremity is observed. This effect has been termed as *kick* after the
 162 works of [18]. On the other hand, when the filament has a finite flexural rigidity
 163 ($K_B = 0.001$ in this simulation), the rolling up of the free end is inhibited, the
 164 *kick* disappears and the flapping amplitude is reduced. Thus, the proposed slender
 165 structure model, incorporating both bending terms and tension, computed to enforce
 166 inextensibility, reproduce thus successfully the same phenomena as the ones observed
 167 in experiments.

168 4 Multiple Flapping Filaments in an Incoming Fluid Flow

169 We consider here the case of two filaments in a *side-by-side* configuration. The non-
 170 dimensional values, the domain size and the initial angles ($\theta = 18^\circ$) are kept the
 171 same as in the case of the single beating filament. According to the experiments of
 172 [3] varying the spacing between filaments d/L leads to the appearance of different
 173 filaments beating regimes. In particular, a symmetrical flapping is observed for dis-
 174 tances $d/L < 0.21$. For higher values, a bifurcation towards a regime characterised
 175 by an out-of-phase flapping is detected. Additionally, the linear stability analyses
 176 carried out in [7, 8] have put forward the existence of three different modes for
 177 such configurations. Therefore, in this context we have considered various scenarios
 178 corresponding to different values of the spacing d/L .

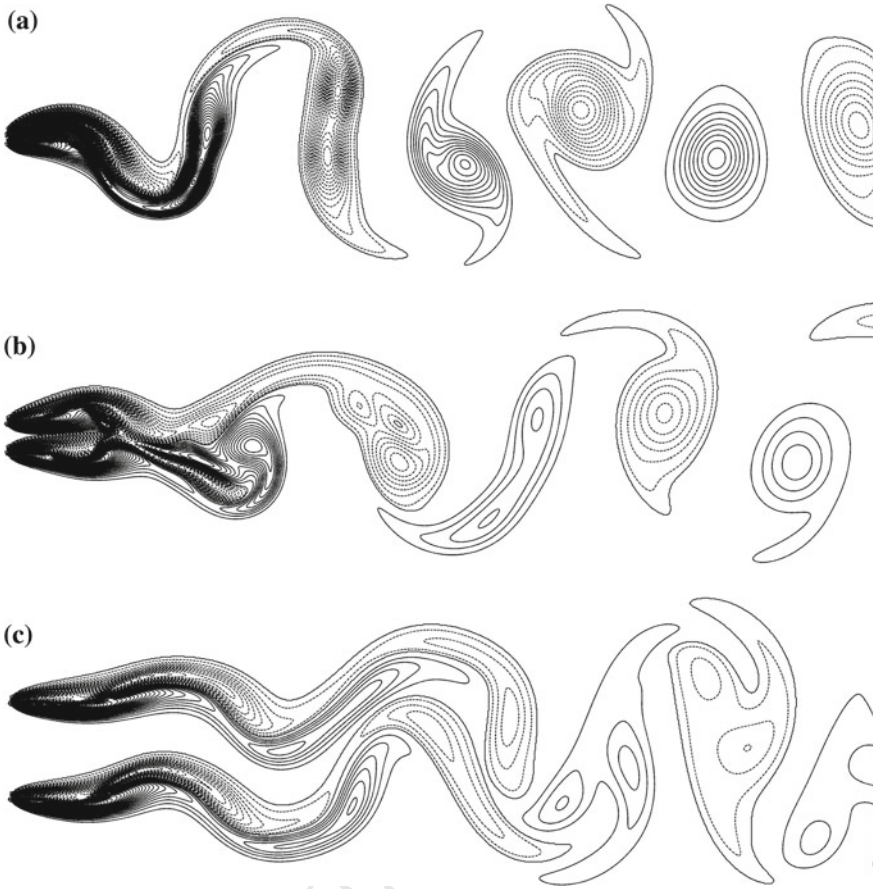


Fig. 3 Snapshots of iso-vorticity for the case of two beating filaments using $\rho = 1.5$, $K_B = 0.001$, $Re = 300$, $Ri = 0.5$ and two different spacings. **a** mode M1 at $d/L = 0.1$, **b** mode M2 at $d/L = 0.3$, **c** mode M2 at $d/L = 1.0$

179 Figure 3 displays the snapshots of iso-vorticity that we predict when considering
 180 three different spacings. The wakes are characterised by a periodic vortex shedding
 181 and by a flapping motion of the filaments (shown in Fig. 4 for the three cases).

- 182 • When the spacing is small ($d/L = 0.1$), we observe the mode M1, where the
 183 filaments are very close to each other and they behave almost as a single thick
 184 filament (see Fig. 3a), resulting in an in-phase beating of the filaments, as displayed
 185 in Fig. 4a.
- 186 • In contrast, when increasing the distance to $d/L = 0.3$, a different behaviour
 187 is observed. This mode (mode M2) is characterised by symmetrical out-of-phase
 188 oscillations, occurring after a transient period going on between $t = 20$ and $t = 60$
 189 (see Fig. 4b). By increasing the filament spacing, the lock-in effect weakens but the

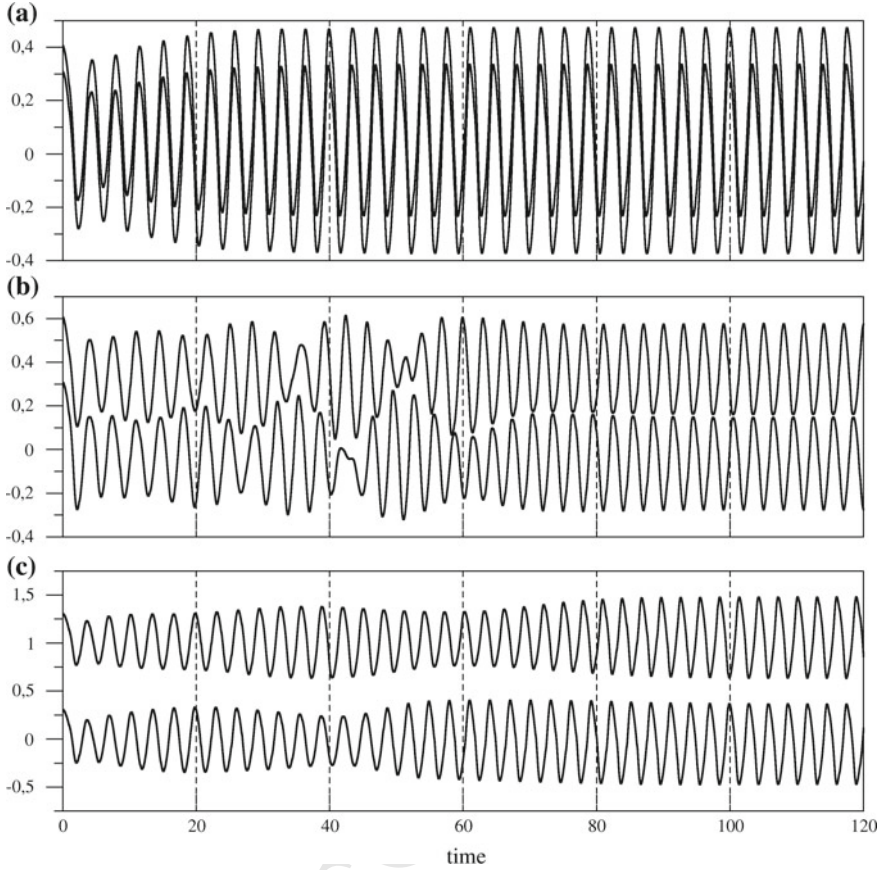


Fig. 4 Time evolution of the y -coordinates of the free extremity of a system of two beating filaments using $\rho = 1.5$, $K_B = 0.001$, $Re = 300$ and $Ri = 0.5$. **a** Mode M1 at $d/L = 0.1$, **b** Mode M2 at $d/L = 0.3$, **c** Mode M2 at $d/L = 1.0$

190 interaction between the wakes generated by each filament still plays a dominant
 191 role, as shown in Fig. 3b. In this regime, the enclosed fluid between both filaments
 192 behaves like a flow generated by a pump due to the out-of-phase flapping, being
 193 compressed when the two free ends approach (which is the case of the snapshot
 194 displayed in Fig. 3b), and released when they move apart.

- 195 • Further increasing the spacing to $d/L = 1$, the wake interaction weakens even
 196 more and the vortex streets behind the filaments decouple (see Fig. 3c). However,
 197 beyond $5L$ downstream of the filaments, the vortices merge into a unique wake
 198 and the filaments reach the mode M2 characterised by an out-of-phase flapping
 199 (see Fig. 4c).
- 200 • If the spacing d/L is further increased, the two filaments eventually reach a totally
 201 decoupled dynamics with an in-phase flapping of the filaments (mode M1).

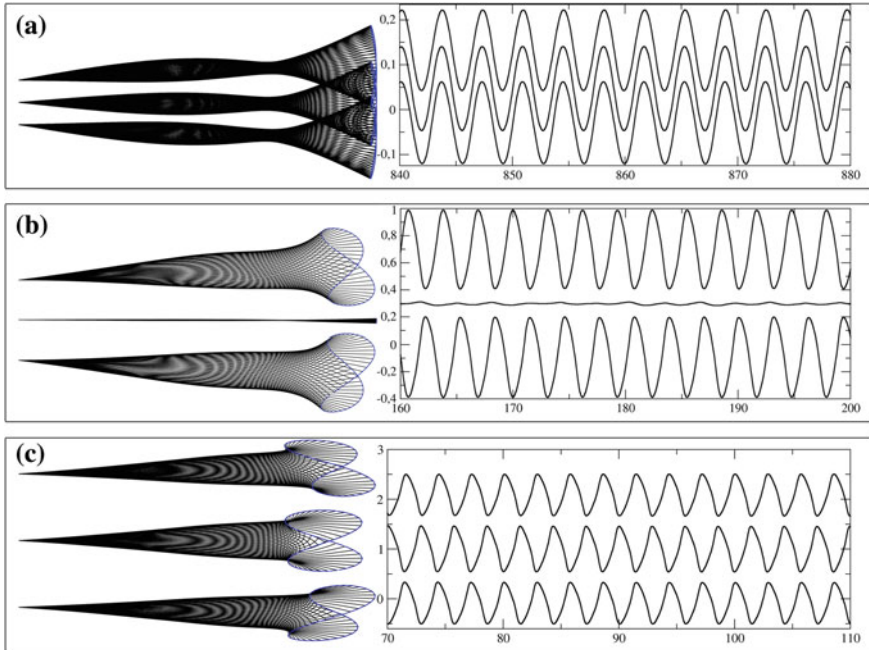


Fig. 5 Flapping patterns in the established regime for the beating of three filaments in a uniform flow for various spacing. **a** Mode M1 at $d/L = 0.05$, **b** mode M2 at $d/L = 0.3$, **c** mode M3 at $d/L = 1.0$. The *solid lines* represent the time evolution of the y-coordinates of the free extremity of each filament, for $\rho = 1.5$, $K_B = 0.001$, $Re = 300$ and $Ri = 0.5$

202 The modal behaviour is consistent with the experimental observations of [3] that
 203 report the onset of the out of phase regime at $d/L = 0.21$, compared to our numerical
 204 predictions indicating a transitory regime occurring between $d/L = 0.21$ and $d/L =$
 205 0.24 .

206 By keeping the same Reynolds number $Re = 300$, the configuration of three fila-
 207 ments placed side-by-side at an initial angle of 0° is investigated. Figure 5 summarizes
 208 the different coupled dynamics obtained with the present simulations. The system
 209 follows the same behaviour as for the case of two filaments, except that a different
 210 beating mode appears:

- 211 • for small spacings ($d/L < 0.1$), the mode M1 is observed, as in the case of two
 212 filaments, where the three filaments are in-phase (mode M1 in Fig. 5a);
- 213 • for $d/L = 0.3$, the two outer filaments flap out of phase while the inner filament
 214 stays almost at rest (mode M2 in Fig. 5b);
- 215 • for large spacing ($d/L = 1.0$) the outer filaments flap in-phase and the inner fila-
 216 ment is out of phase (mode M3 in Fig. 5c);
- 217 • as for the case of two filaments, mode M1 is observed for very large spacing
 218 ($d/L > 4.0$) with an in-phase flapping of the three filaments.

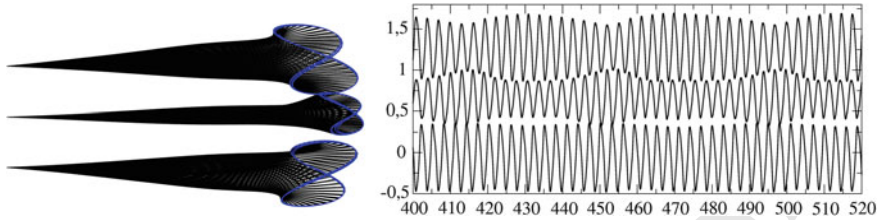


Fig. 6 Transition mode observed between M2 and M3 for $d/L = 0.6$. The *solid lines* represent the time evolution of the y -coordinates of the free extremity of each filament, for $\rho = 1.5$, $K_B = 0.001$, $Re = 300$ and $Ri = 0.5$

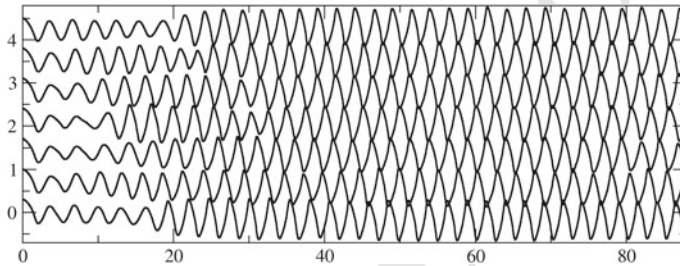


Fig. 7 Time evolution of the y -coordinates of the free extremity of a system of seven beating filaments using $\rho = 1.5$, $K_B = 0.001$, $Re = 300$ and $Ri = 0.5$

219 Additionally, we observed for $d/L = 0.6$ a transition mode characterised by the same
 220 behaviour as mode M3 but with a low frequency modulation in the amplitude of the
 221 flapping of the filaments, as shown in Fig. 6.

222 This transition mode has also been reported in the numerical study of [19]. In their
 223 simulations at $Re = 100$, they also point out another transitional mode where the
 224 inner filament is flapping at a frequency reduced by half compared to outer filaments,
 225 which we don't observe in our simulations at $Re = 300$.

226 When more than three filaments are considered, the system is expected to exhibit
 227 more transitory modes resulting from the coupling between the described baseline
 228 modes (M1, M2 and M3). Figure 7 displays for instance a mode similar to mode M3
 229 obtained for seven flapping filaments with a spacing of $d/L = 0.7$.

230 5 Concluding Remarks

231 We have shown that a simple structural model of a flexible slender structure including
 232 its flexural rigidity, the tension (enforcing inextensibility) and the added mass can
 233 successfully capture numerically the dynamics of a flapping filament immersed in
 234 an uniform incoming flow. When considering two filaments placed side-by-side, the
 235 wake interactions and the modal behaviour of the system have been captured cor-
 236 rectly, in agreement with the predictions of linear stability analysis and experiments.

237 However, we have only considered here the influence of the filament spacing, but
 238 as pointed out by the study of [8], the influence of the added mass $\Delta\rho$ plays also a
 239 significant role.

240 For the case of three filaments, a set of three baseline modes have been highlighted:
 241 in-phase flapping (M1), out-of-phase flapping with the inner filament at rest (M2),
 242 in-phase flapping with the inner filament flapping out of phase (M3). For the general
 243 case of a layer made of N filaments, one would expect the system to be characterised
 244 by the appearance of N baseline modes originating from the combination of the M1,
 245 M2 and M3 baseline ones consistently with the theoretical prediction of [8].

246 Close-term perspectives of this work will be focussed on the shape adaptation
 247 properties and modal behavior of a layer of filaments flapping in three dimensions,
 248 within the scope of flow control applications.

249 **Acknowledgments** The authors acknowledge the financial help of the *PELskin* European project
 250 (FP7 AAT.2012.6.3-1). This work was partially supported by the Spanish Ministry of Economics
 251 through the grant DPI2010-20746-C03-02.

252 References

- 253 1. Païdoussis, M.P.: Fluid-Structure Interactions: Slender Structures and Axial Flow, vol. 2. Else-
 254 vier Academic Press, Cambridge (2004)
- 255 2. Shelley, M.J., Zhang, J.: Flapping and bending bodies interacting with fluid flows. *Ann. Rev.*
 256 *Fluid Mech.* **43**(1), 449–465 (2011)
- 257 3. Zhang, J., Childress, S., Libchaber, A., Shelley, M.: Flexible filaments in a flowing soap film
 258 as a model for one-dimensional flags in a two-dimensional wind. *Nature* **408**, 835–839 (2000)
- 259 4. Zhu, L., Peskin, C.S.: Interaction of two flapping filaments in a flowing soap film. *Phys. Fluids*
 260 **15**, 1954–1960 (2000)
- 261 5. Pinelli, A., Naqavi, I.Z., Piomelli, U., Favier, J.: Immersed-boundary methods for general
 262 finite-difference and finite-volume navier-stokes solvers. *J. Comput. Phys.* **229**(24), 9073–9091
 263 (2010)
- 264 6. Domenichini, F.: On the consistency of the direct forcing method in the fractional step solution
 265 of the navier-stokes equations. *J. Comput. Phys.* **227**(12), 6372–6384 (2008)
- 266 7. Schouweiler, L., Eloy, C.: Coupled flutter of parallel plates. *Phys. Fluids* **21**, 081703 (2009)
- 267 8. Michelin, S., Llewellyn Smith, S.G.: Linear stability analysis of coupled parallel flexible plates
 268 in an axial flow. *J. Fluids Struct.* **25**(7), 1136–1157 (2009)
- 269 9. Favier, J., Dauptain, A., Basso, D., Bottaro, A.: Passive separation control using a self-adaptive
 270 hairy coating. *J. Fluid Mech.* **627**, 451 (2009)
- 271 10. Favier, J., Revell, A., Pinelli, A.: A lattice boltzmann—immersed boundary method to simulate
 272 the fluid interaction with moving and slender flexible objects. HAL, hal(00822044) (2013)
- 273 11. Succi, S.: *The Lattice Boltzmann Equation*. Oxford University Press, New York (2001)
- 274 12. Bhatnagar, P., Gross, E., Krook, M.: A model for collision processes in gases. i: small amplitude
 275 processes in charged and neutral one-component system. *Phys. Rev.* **94**, 511–525 (1954)
- 276 13. Qian, Y., D’Humières, D., Lallemand, P.: Lattice bgk models for navier-stokes equation. *Euro-*
 277 *phys. Lett.* **17**(6), 479–484 (1992)
- 278 14. Guo, Z., Zheng, C., Shi, B.: Discrete lattice effects on the forcing term in the lattice boltzmann
 279 method. *Phys. Rev. E* **65**, 046308 (2002)
- 280 15. Zhu, L., Peskin, C.S.: Simulation of a flapping flexible filament in a flowing soap film by the
 281 immersed boundary method. *Phys. Fluids* **179**, 452–468 (2002)

- 282 16. Huang, W.-X., Shin, S.J., Sung, H.J.: Simulation of flexible filaments in a uniform flow by the
283 immersed boundary method. *J. Comput. Phys.* **226**(2), 2206–2228 (2007)
- 284 17. Bagheri, Shervin, Mazzino, Andrea, Bottaro, Alessandro: Spontaneous symmetry breaking of
285 a hinged flapping filament generates lift. *Phys. Rev. Lett.* **109**, 154502 (2012)
- 286 18. Bailey, H.: Motion of a hanging chain after the free end is given an initial velocity. *Am. J. Phys.*
287 **68**, 764–767 (2000)
- 288 19. Tian, F.-B., Luo, H., Zhu, L., Lu, X.-Y.: Coupling modes of three filaments in side-by-side
289 arrangement. *Phys. Fluids* **23**(11), 111903 (2011)

UNCORRECTED PROOF

Author Queries

Chapter 10

Query Refs.	Details Required	Author's response
	No queries.	

UNCORRECTED PROOF

MARKED PROOF

Please correct and return this set

Please use the proof correction marks shown below for all alterations and corrections. If you wish to return your proof by fax you should ensure that all amendments are written clearly in dark ink and are made well within the page margins.

<i>Instruction to printer</i>	<i>Textual mark</i>	<i>Marginal mark</i>
Leave unchanged	... under matter to remain	Ⓟ
Insert in text the matter indicated in the margin	∧	New matter followed by ∧ or ∧ [Ⓢ]
Delete	/ through single character, rule or underline or ┌───┐ through all characters to be deleted	Ⓞ or Ⓞ [Ⓢ]
Substitute character or substitute part of one or more word(s)	/ through letter or ┌───┐ through characters	new character / or new characters /
Change to italics	— under matter to be changed	↵
Change to capitals	≡ under matter to be changed	≡
Change to small capitals	≡ under matter to be changed	≡
Change to bold type	~ under matter to be changed	~
Change to bold italic	≈ under matter to be changed	≈
Change to lower case	Encircle matter to be changed	≡
Change italic to upright type	(As above)	⊕
Change bold to non-bold type	(As above)	⊖
Insert 'superior' character	/ through character or ∧ where required	Υ or Υ under character e.g. Υ or Υ
Insert 'inferior' character	(As above)	∧ over character e.g. ∧
Insert full stop	(As above)	⊙
Insert comma	(As above)	,
Insert single quotation marks	(As above)	Ƴ or ƴ and/or Ƶ or ƶ
Insert double quotation marks	(As above)	ƴ or ƶ and/or Ƶ or Ʒ
Insert hyphen	(As above)	⊥
Start new paragraph	┌	┌
No new paragraph	┐	┐
Transpose	└┐	└┐
Close up	linking ○ characters	Ⓞ
Insert or substitute space between characters or words	/ through character or ∧ where required	Υ
Reduce space between characters or words		↑